

# A Study of the Interactions in an Extended Unsupported Gold-Silver Chain

Eduardo J. Fernández,<sup>[a]</sup> Antonio Laguna,<sup>\*[b]</sup> José M. López-de-Luzuriaga,<sup>[a]</sup>  
Miguel Monge,<sup>[a]</sup> Pekka Pyykkö,<sup>\*[c]</sup> and Nino Runeberg<sup>[c]</sup>

**Keywords:** Gold / Silver / Ab initio calculations / N ligands

The complex  $[\text{Ag}(\text{Py})_3][\text{Au}(\text{C}_6\text{F}_5)_2]\cdot\text{Py}$  (**1**) (Py = pyridine) has been prepared by the reaction of  $\text{NBu}_4[\text{Au}(\text{C}_6\text{F}_5)_2]$  with  $\text{AgClO}_4$  in the presence of pyridine. The crystallographic measurements indicate the presence of an extended unsupported one-dimensional chain of alternating gold and silver atoms. This arrangement is due to the formation of molecular Au–Ag ion pairs, to the  $\pi$ -stacking of  $\text{C}_6\text{F}_5$  and pyridine arene ligands and to the packing effects that lead to molecular

ion pairs at short distance. Theoretical calculations based on approximate experimental distances and angles reveal the presence of both metallophilic  $\text{Au}^1\text{–Ag}^1$  and aromatic  $\text{C}_6\text{F}_5$ -pyridine interactions. From a theoretical point of view the nature of the intermetallic attraction arises from both an ionic contribution and from dispersion-type correlation effects; the aromatic interaction is mainly due to dispersion-type correlation effects.

## Introduction

The tendency of gold centers to aggregate has been termed “aurophilicity” by Schmidbaur.<sup>[1]</sup> Many research groups have been involved in an exhaustive search for structural information concerning such systems. The results have encouraged the theorists to construct theoretical models whose results could be compared with the experimental data. These models lead one to conclude that these interactions arise from correlation and relativistic effects.<sup>[2,3]</sup> The attraction due to electron correlation is dominated by dispersion, with a significant contribution from the recently identified ionic-type excitations.<sup>[4]</sup> These studies are nowadays being extended to other metals with closed shell configurations in theoretical models of systems with the same or different centers. Previous studies carried out in our group of heteropolynuclear metallacycles of the type  $[\text{AuM}(\text{HSCH}_2\text{PH}_2)_2]^{2+}$  (M = Ag, Cu) concluded that the presence of only one gold atom is enough to induce metallophilic attractions in the group congeners and that this effect could be modulated depending on the gold ligand.<sup>[5]</sup> We also performed a detailed analysis of the  $d^8\text{–}d^{10}$  interaction between  $\text{Pd}^{\text{II}}$  and  $\text{Au}^{\text{I}}$  in the model complex  $[\text{AuPdCl}_3(\text{HSCH}_2\text{PH}_2)_2]$  showing a dominant dispersion effect, some ionic contributions and no net charge transfer

between the metals.<sup>[6]</sup> In both cases a bidentate ligand acts as a bridge between the metallic centers and its contribution to the close approach of the metal atoms cannot be neglected.

In contrast, the anionic complex  $[\text{Au}(\text{C}_6\text{F}_5)_2]^-$  has been found to be a very valuable agent in the preparation of heteropolynuclear complexes in which the metal-metal interactions are not imposed by the ligand architecture.<sup>[7–10]</sup> Accordingly, we report here the synthesis, characterization and theoretical study of the complex  $[\text{Ag}(\text{Py})_3][\text{Au}(\text{C}_6\text{F}_5)_2]\cdot\text{Py}$  (**1**) (Py = pyridine), which shows an extended unsupported one-dimensional chain formed by repetition of gold-silver ion pairs that, in addition, displays  $\pi$ -stacking interactions<sup>[11–14]</sup> between  $\text{C}_6\text{F}_5$  and pyridine arene ligands supporting the formation of the infinite chains.

## Results and Discussion

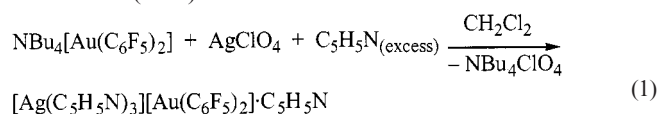
Compound **1** was synthesized according to Equation (1). An ionic formulation could be proposed in solution based on the molar conductivity measurement in acetone solution ( $\Lambda_{\text{M}} = 110 \text{ } \Omega^{-1} \text{ cm}^2 \text{ mol}^{-1}$ ,  $5 \cdot 10^{-4} \text{ M}$ ) assigned to a 1:1 electrolyte. The IR spectrum shows, amongst others, the absorptions of the  $\text{C}_6\text{F}_5$  ligands at 783, 963 and  $1500 \text{ cm}^{-1}$ <sup>[15]</sup> and pyridine ligands in the range  $617\text{–}651 \text{ cm}^{-1}$ .<sup>[16]</sup> Moreover, the  $^{19}\text{F}$  NMR chemical shifts of  $\delta = -114.60$ ,  $-162.07$  and  $-163.87$  are similar to the values observed for the  $[\text{Au}(\text{C}_6\text{F}_5)_2]^-$  fragment in solution. The separation of compound **1** into ionic components in solution is also confirmed by the mass spectrometry measurements (electrospray) in which we observe, depending on the experiment, the  $[\text{Au}(\text{C}_6\text{F}_5)_2]^-$  anion at  $m/z = 541$  ( $\text{ES}^-$ ) and the

<sup>[a]</sup> Departamento de Química, Universidad de la Rioja-UA-CSIC Madre de Dios, 51, 26004 Logroño, Spain

<sup>[b]</sup> Departamento de Química Inorgánica, Instituto de Ciencia de Materiales de Aragón, Universidad de Zaragoza-CSIC 50009 Zaragoza, Spain  
E-mail: alaguna@posta.unizar.es

<sup>[c]</sup> Department of Chemistry, University of Helsinki, P. O. B. 55 (A. I. Virtasen aukio 1), 00014 Helsinki, Finland  
E-mail: pekka.pyykko@helsinki.fi

$[\text{Ag}(\text{Py})_2]^+$  cation at  $m/z = 266$  or the  $[\text{Ag}(\text{Py})]^+$  cation at  $m/z = 187$  ( $\text{ES}^+$ ).



A single-crystal X-ray diffraction study has been carried out for compound **1**. The silver atom is found to be disordered over two positions (50% each one), which makes the results of this study not completely valid. Despite this, the molecular structure can be described as being formed by  $[\text{Au}(\text{C}_6\text{F}_5)_2]^-$  units and tricoordinate  $[\text{Ag}(\text{Py})_3]^+$  cations giving rise to a molecular ion-pair model (Figure 1). The molecular Au–Ag ion pairs are repeated in one dimension forming a chain due to the presence of  $\pi$ -stacking interactions between  $\text{C}_6\text{F}_5$  and pyridine rings and packing effects. Because of the disorder, any comment about bond lengths and angles is inappropriate, but nevertheless, the singular structural disposition could be used as a basis for a theoretical study.

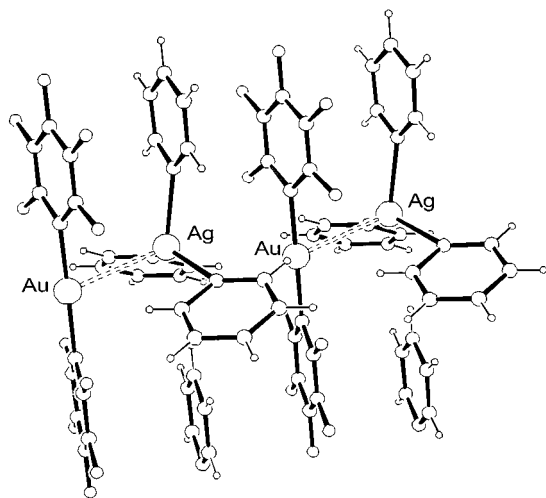


Figure 1. Structure of complex **1**; two molecular Au–Ag ion pairs and  $\text{C}_6\text{F}_5$ -pyridine  $\pi$ -stacking are shown

The structural arrangement of complex **1** shows some interesting features from a theoretical point of view. First, a short distance between the  $\text{Au}^I$  and  $\text{Ag}^I$  atoms is observed. Secondly, two  $\text{C}_6\text{F}_5 \cdots \text{Py}$  aromatic interactions could be proposed in the formula unit  $[\text{Ag}(\text{Py})_3][\text{Au}(\text{C}_6\text{F}_5)_2]\cdot\text{Py}$ , one between a free pyridine molecule and one of the  $\text{C}_6\text{F}_5$  rings and the other between a pyridine ligand bonded to silver and the other  $\text{C}_6\text{F}_5$  ring. A theoretical study of these secondary interactions has been carried out separately on three different model systems (Figure 2) using two levels of theory based on Hartree–Fock (HF) and Local second order Møller–Plesset perturbation (LMP2) theory. The LMP2 approach, which is the simplest of the local correlation methods,<sup>[17–19]</sup> is analogous to the traditional MP2 but is performed using localized occupied and local virtual orbitals. The virtual space is spanned by nonorthogonal atomic orbitals (AOs), which are projected against the occu-

ried space in order to ensure orthogonality between the occupied and virtual spaces. These nonorthogonal projected orbitals are inherently localized. The *orbital domain* [i] is that part of the virtual space assigned to an individual LMO (i), consisting only of those basis functions that are centered on the atoms involved in that particular LMO. The orbital domains [i] are kept orthogonal to the occupied space by projecting out the LMOs. Double excitations from an orbital pair (ij) are only allowed into the *pair domain* [ij], which is spanned by the union of the corresponding orbital domains [i] and [j]. The introduction of this physically appealing restriction in which electron pairs are only interacting in the vicinity of either electron, gives rise to the significant reduction of the computational cost as well as a diminished basis-set supposition error (BSSE). On the other hand the use of localized orbitals makes it possible to decompose the correlation contribution into the interaction energy of a complex according to different classes of double excitations. The two most important contributions arise from the dispersion class, in which one electron is excited from each subsystem into its own virtual space, and the ionic class, in which one of the electrons is excited from one of the subsystems to the virtual space of the other subsystem. In addition to the partition of the correlation contribution of the interaction energy, we can assume that the major part of the electrostatic interaction is already described at the uncorrelated HF level. Hence, we can theoretically study in great detail the forces that are responsible for the one dimensional disposition of complex **1** in the solid state.

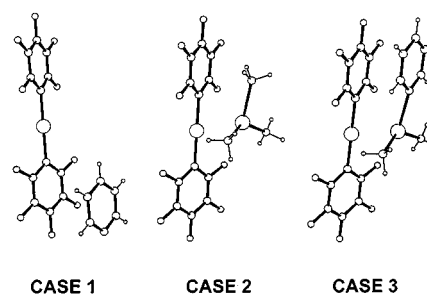


Figure 2. The assumed structures of the theoretical models, (a):  $[\text{Au}(\text{C}_6\text{F}_5)_2] \cdots \text{Py}$  CASE 1; (b):  $[\text{Ag}(\text{NH}_3)_3] \cdots [\text{Au}(\text{C}_6\text{F}_5)_2]$  CASE 2; (c):  $[\text{Ag}(\text{NH}_3)_2(\text{Py})] \cdots [\text{Au}(\text{C}_6\text{F}_5)_2]$  CASE 3

Finally, we emphasize that the role of dynamic correlation effects in transition-metal chemistry is well-known. The particular correlation effects leading to the  $R^{-6}$  dispersion forces involve dipole-allowed virtual excitations at the two centers involved ( $A \rightarrow A'$ ,  $B \rightarrow B'$ ). The “ionic correlation” mentioned above means ( $A \rightarrow A'$ ,  $B \rightarrow A'$ ). These interaction can only be reproduced by explicitly correlated methods.

One advantage of the LMP2 method is that it has almost no BSSE. Thus, no counterpoise corrections are needed.

In principle one should simulate the entire crystal structure but we have only considered particular contributions using cluster models.

In case 1 (Figure 2a) we have studied the interaction between  $[\text{Au}(\text{C}_6\text{F}_5)_2]^-$  and a free pyridine molecule present in the crystal structure. The results of this interaction are given in Table 1 and the calculated interaction energy curves are shown in Figure 3. The HF curve is repulsive, whereas the LMP2 curve is attractive. The calculated  $[\text{Au}(\text{C}_6\text{F}_5)_2] \cdots \text{Py}$  distance, defined as the distance between the virtually parallel Py and  $\text{C}_6\text{F}_5$  units, is 344.7 pm for our simplified model system and the interaction energy is 36.5 kJ/mol at the equilibrium distance. Thus, we can assume that the aromatic interaction between a  $\text{C}_6\text{F}_5$  group from the  $[\text{Au}(\text{C}_6\text{F}_5)_2]^-$  unit and the free pyridine molecule is due to dispersion-type correlation effects, since a stabilization energy is observed when these effects are included at the LMP2 level of theory and a repulsion between the rings at HF level is found.

Table 1. Optimized distance ( $R_e$ ) and interaction energy ( $E_e$ ) for the three model systems at HF and LMP2 levels (distances in pm and energy in kJ/mol)

	$R_e$ (SCF)	$E_e$ (SCF)	$R_e$ (LMP2)	$E_e$ (LMP2)
CASE 1	REPULSIVE	-0.44 <sup>[a]</sup>	317.8 <sup>[b]</sup>	36.5
CASE 2	312.3	160	284.3	234
CASE 3	323.2	143	289.4	239

<sup>[a]</sup> At the LMP2 optimized distance. <sup>[b]</sup> Referred to the Au–Ag distance.

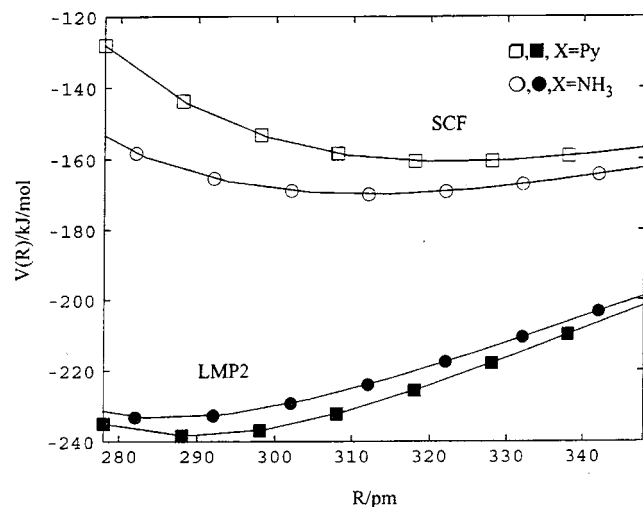


Figure 3. Interaction energy curves for the  $[\text{Au}(\text{C}_6\text{F}_5)_2] \cdots [\text{XAg}(\text{NH}_3)_2]$  ( $X = \text{NH}_3, \text{Py}$ ) interaction calculated at the SCF and LMP2 levels

Many earlier examples of coplanar “ $\pi$ -stacks” between aromatic rings are known. A typical ring-ring distance is 350 pm.<sup>[13]</sup> If the two rings have opposite electric quadrupole moments, like  $\text{C}_6\text{H}_6$  and  $\text{C}_6\text{F}_6$ , the electric quadrupole-quadrupole interactions already yield an attraction of about 6 kJ/mol.<sup>[20]</sup> Examples of  $\pi$ -stacks in organometallic chemistry are also known.<sup>[14]</sup> For further information on this subject see ref.<sup>[21]</sup>

In case 2 (Figure 2b) we have proposed a model system  $[\text{Ag}(\text{NH}_3)_3] \cdots [\text{Au}(\text{C}_6\text{F}_5)_2]$  in order to study only the intermetallic Au–Ag interaction. The results of the interaction energies at the theoretically predicted equilibrium distance are given in Table 1 and the calculated interaction energy curves are shown in Figure 3. In this case, the HF curve is attractive with a minimum corresponding to the equilibrium distance at 312.3 pm and an attractive interaction energy of 160 kJ/mol compared to the ionic dissociation limit. Regarding the LMP2 curve we also obtain an attractive behavior with an interaction energy at the equilibrium distance (284.3 pm) of 234 kJ/mol. In this case, in which only the Au $\cdots$ Ag interaction is studied, both electrostatic attraction and dispersion-type correlation effects are responsible for this interaction. The electrostatic interaction is responsible for the attractive behavior obtained at the HF level since dispersion-type correlation effects are not included. The additional stabilization obtained at the LMP2 level is due to the introduction of these correlation effects, which include dispersion.

Going from case 2 to case 3, we exchange one of the  $\text{NH}_3$  ligands bonded to silver for one pyridine ligand that is parallel and at a short distance from one of the  $\text{C}_6\text{F}_5$  rings bonded to gold (Figure 2c). In this case we study the influence of the presence of two interactions, the intermetallic Au–Ag and the aromatic  $\text{C}_6\text{F}_5 \cdots \text{Py}$  (Ag-bonded), at the equilibrium distances and at the interaction energy values. For this case we obtain an  $\text{Au}^{\text{I}} \cdots \text{Ag}^{\text{I}}$  equilibrium distance at the HF level of 323.2 pm and of 289.4 pm at the LMP2 level. The equilibrium distance at both levels of theory is accompanied by interaction energy values of 143 kJ/mol at the HF level and 239 kJ/mol at the LMP2 level (see Table 2 and Figure 3). Thus, this comparison allows us, if we make the simplified conclusion that HF covers electrostatic interactions and the correlation energy (the difference between LMP2 and HF) covers the dispersion contribution, to establish that the overall interaction is very similar for both cases 2 and 3, in terms of the LMP2 equilibrium distance and the interaction energy (284.3 pm and 234 kJ/mol for case 2 and 289.4 pm and 239 kJ/mol for case 3). However, the contributions are different. The pyridine ligand in case 3 introduces electrostatic repulsion since the electrostatic interaction diminishes from 160 kJ/mol in case 2 to 143 kJ/mol in case 3, but it also introduces attractive dispersion interactions (74 kJ/mol in case 2 to 96 kJ/mol in case 3), as occurs in case 1. In Table 2 we compare the results for cases 2 and 3 at the LMP2 optimized distances, which are quite similar in both cases (284 vs. 289 pm respectively).

Table 2. Electrostatic (HF) and dispersion (LMP2) contributions to the intermetallic Au–Ag interaction (kJ/mol) at the LMP2 optimized distance

	Electrostatic	Correlation Energy	Total
CASE 2	160	74	234
CASE 3	143	96	239

The partitioning of the correlation contribution to the  $[\text{Ag}(\text{NH}_3)_3] \cdots [\text{Au}(\text{C}_6\text{F}_5)_2]$  (case 2) and  $[\text{Ag}(\text{NH}_3)_2(\text{Py})] \cdots [\text{Au}(\text{C}_6\text{F}_5)_2]$  (case 3) interaction energies based on the obtained experimental distances are given in Table 3. The introduction of the pyridine ring into the model system in case 3 gives, as we have commented above, a net enhancement of the correlation energy and, looking at the partition of this correlation energy, the dispersion (van der Waals) contribution increases with respect to the ionic correlation contribution seen as the charge transfer.

Table 3. LMP2 correlation energy partitioning at the experimental geometry (kJ/mol)

	Ex-dispersion	Dispersion	Ionic	Ag→Au	Au→Ag
CASE 2	0.0	29	16	4	12
CASE 3	-0.1	45	20	6	14

## Conclusions

1) An ionic, Coulomb attraction obviously exists between the  $[\text{Au}(\text{C}_6\text{F}_5)_2]^-$  anions and the  $[\text{Ag}(\text{Py})_3]^+$  cations. This is an important contribution behind the infinite chains.

2) In addition, dispersion-type correlation effects lead to attractions both between  $\text{Ag}^I$  and  $\text{Au}^I$  and between  $\text{C}_6\text{F}_5$  and pyridine moieties.

3) Looking at the detailed correlation energy partitioning, the most important contributions are the normal dispersion (van der Waals) terms. Charge-transfer-type contributions are about one third as important and, of them, the Au→Ag virtual excitation is more important than the Ag→Au one.

## Experimental Section

**General:** All experiments were performed under argon by using standard Schlenk techniques. Solvents were dried and distilled under argon.  $^1\text{H}$  and  $^{19}\text{F}$  NMR spectra were recorded on a Bruker ARX 300. Elemental analyses were carried out with a C.E. instrument EA-1110 CHNS-O microanalyzer. Infrared spectrum was recorded in the  $4000\text{--}200\text{ cm}^{-1}$  range on a Perkin-Elmer FT-IR Spectrum 1000 spectrophotometer as nujol mulls between polyethylene sheets. Mass spectra were recorded on a HP-5989B Mass Spectrometer API-Electrospray with interface 59987A.

**$[\text{Ag}(\text{Py})_3][\text{Au}(\text{C}_6\text{F}_5)_2]\cdot\text{Py}$  (1):** The reaction between  $\text{NBu}_4[\text{Au}(\text{C}_6\text{F}_5)_2]$  (200 mg, 0.258 mmol),  $\text{AgClO}_4$  (54 mg, 0.258 mmol) and an excess of pyridine in  $\text{CH}_2\text{Cl}_2$  leads, after a slow crystallization process (24 h) at low temperature, to compound **1** as colorless crystals. Yield: 47%.  $^1\text{H}$  NMR  $[(\text{CD}_3)_2\text{CO}]$ :  $\delta = 7.52$  (dd, 2 H, -CH-), 7.96 (t, 1 H, -CH-), 8.67 (d, 2 H, -CH-).  $\text{C}_{32}\text{H}_{20}\text{AgAuF}_{10}\text{N}_4$  (955.4): calcd. C 40.23, H 2.18, N 5.86; found C 39.92, H 2.25, N 5.41.

**Computational Details:** All calculations were performed as implemented in the MOLPRO program package. For the metals, the 19 valence electron pseudopotentials from Stuttgart and the corresponding basis sets<sup>[22a]</sup> augmented with two f polarization functions were used.<sup>[22b]</sup> For the lighter atoms the cc-pVDZ basis sets were used.<sup>[22c]</sup> The LMOs were obtained through a Pipek–Mezey localization procedure.<sup>[22d]</sup>

## Acknowledgments

This work was supported by the Spanish DGES (BQU2001-2409) and the U.R. API-01/B14. P. Pyykkö and N. Runeberg are supported by The Academy of Finland.

- [1] F. Scherbaum, A. Grohmann, B. Huber, C. Krüger, H. Schmidbaur, *Angew. Chem. Int. Ed. Engl.* **1988**, *27*, 1544–1546.  
 [2] P. Pyykkö, Y.-F. Zhao, *Angew. Chem. Int. Ed. Engl.* **1991**, *30*, 604–605.  
 [3] P. Pyykkö, T. Tamm, *Organometallics* **1998**, *17*, 4842–4852.  
 [4] N. Runeberg, M. Schütz, H.-J. Werner, *J. Chem. Phys.* **1999**, *110*, 7210–7215.  
 [5] E. J. Fernández, J. M. López-de-Luzuriaga, M. Monge, M. A. Rodríguez, O. Crespo, M. C. Gimeno, A. Laguna, P. G. Jones, *Chem. Eur. J.* **2000**, *6*, 636–644.  
 [6] O. Crespo, A. Laguna, E. J. Fernández, J. M. López-de-Luzuriaga, P. G. Jones, M. Teichert, M. Monge, P. Pyykkö, N. Runeberg, M. Schütz, H.-J. Werner, *Inorg. Chem.* **2000**, *39*, 4786–4792.  
 [7] R. Usón, A. Laguna, M. Laguna, P. G. Jones, G. M. Sheldrick, *J. Chem. Soc., Chem. Commun.* **1981**, 1097–1098.  
 [8] R. Usón, A. Laguna, M. Laguna, B. R. Manzano, P. G. Jones, G. M. Sheldrick, *J. Chem. Soc., Dalton Trans.* **1984**, 285–292.  
 [9] O. Crespo, E. J. Fernández, P. G. Jones, A. Laguna, J. M. López-de-Luzuriaga, A. Mendía, M. Monge, E. Olmos, *Chem. Commun.* **1998**, 2233–2234.  
 [10] E. J. Fernández, M. C. Gimeno, A. Laguna, J. M. López-de-Luzuriaga, M. Monge, P. Pyykkö, D. Sundholm, *J. Am. Chem. Soc.* **2000**, *122*, 7287–7293.  
 [11] W. L. Jorgensen, D. L. Severance, *J. Am. Chem. Soc.* **1990**, *112*, 4768–4774.  
 [12] D. D. Graf, J. P. Campbell, L. L. Miller, K. R. Mann, *J. Am. Chem. Soc.* **1996**, *118*, 5480–5481.  
 [13] D. D. Graf, R. G. Duan, J. P. Campbell, L. L. Miller, K. R. Mann, *J. Am. Chem. Soc.* **1997**, *119*, 5888–5899.  
 [14] G. Ujaque, F. Maseras, A. Lledós, *J. Am. Chem. Soc.* **1999**, *121*, 1317–1323.  
 [15] R. Usón, A. Laguna, J. García, M. Laguna, *Inorg. Chim. Acta* **1979**, *37*, 201–207.  
 [16] K. Nakamoto, *Infrared and Raman Spectra of Inorganic and Coordination Compounds*, 4th Edition, John Wiley & Sons, **1986**, p. 206.  
 [17] P. Pulay, *Chem. Phys. Lett.* **1983**, *100*, 151–154.  
 [18] S. Saebø, P. Pulay, *Annu. Rev. Phys. Chem.* **1993**, *44*, 213–236.  
 [19] C. Hampel, H.-J. Werner, *J. Chem. Phys.* **1996**, *104*, 6286–6297.  
 [20] N. J. Heaton, P. Bello, B. Herradón, A. del Campo, J. Jiménez-Barbero, *J. Am. Chem. Soc.* **1998**, *120*, 12371–12384.  
 [21] D. Sundholm, M. R. Sundberg, R. Uggla, *J. Phys. Chem. A* **1998**, *102*, 7137–7142.  
 [22] [22a] D. Andrae, U. Häusserman, M. Dolg, H. Stoll, H. Preuss, *Theor. Chim. Acta* **1990**, *77*, 123–141. [22b] P. Pyykkö, N. Runeberg, F. Mendizabal, *Chem. Eur. J.* **1997**, *3*, 1451–1457. [22c] T. H. Dunning, Jr., *J. Chem. Phys.* **1989**, *90*, 1007–1023. [22d] J. Pipek, P. G. Mezey, *J. Chem. Phys.* **1989**, *90*, 4916–4926.

Received August 2, 2001

[I01285]